RSC Advances

PAPER

View Article Online
View Journal | View Issue

Cite this: RSC Adv., 2016, 6, 28570

The corrosion behaviors of multilayer diamond-like carbon coatings: influence of deposition periods and corrosive medium†

Mingjun Cui,[ac] Jibin Pu,[b] Guangan Zhang,[a] Liping Wang*[ab] and Qunji Xue*[ab]

Received 2nd March 2016
Accepted 7th March 2016

DOI: 10.1039/c6ra05527c

www.rsc.org/advances

Electrochemical measurements, salt spray tests and immersion tests were employed to investigate the influence of deposition periods and corrosive medium (NaCl, H_2SO_4, HCl, NaOH) on the corrosion behaviors of silicon doped multilayer diamond-like carbon (DLC) coatings. The results showed that the corrosion resistance of the multilayer DLC coatings was significantly improved with the increase of deposition periods. Interestingly, the coating with the highest deposition periods provided good corrosion protection in neutral and acidic solutions while poor corrosion protection in alkaline and acidic chloride solutions.

1. Introduction

Diamond-like carbon (DLC) coatings have stimulated extensive research interest as surface coatings for improving corrosion protection owing to their unique characteristics such as electrical resistivity, chemical inertness and exceptional mechanical characteristics.[1–5] Particularly, DLC coatings were chemically resistant to any solvent such as acid, alkali or organic solvent, which made them become a promising candidate for improving corrosion protection to a steel substrate.[6,7] Unfortunately, in spite of having excellent corrosion resistance, the high internal stress limited its thickness, and frequently led to debonding, cracking or delamination of the coating from the substrate, which limited the practical application of DLC coatings.[3,4,7–9] Many approaches had been applied to minimize the residual stress and improve the corrosion resistance of DLC coatings, for instance, functional grading,[10] doping[9,11] and multilayer structure.[3,4,12] Wherein, multilayer structure was one effective method to relieve the internal stress and reduce the defect density, leading to the improvement of corrosion protection to steel substrate.[5,7,12,13] On one hand, the tensile stress and compressive stress in the coating could reach equilibrium owing to the multilayer structure.[12] On the other hand, the alternating structure showed better possibility to reduce corrosion causes, extend or block the aggressive agents' path by interrupting the through-thickness pinholes.[14–16]

Wang *et al.*[5] developed a multilayer DLC coating (alternate SiC and DLC layers) on mild steel, and found that this coating was effective to prevent the substrate from long-term corrosion attack and scale formation. Uematsu *et al.*[7] prepared the multilayer DLC coatings which successfully removed the through-film thickness defects and improved the corrosion fatigue strength under aggressive environments. It was evident that researchers had demonstrated the feasibility of multilayer DLC coatings in protecting the substrates from the corrosion attack. However, the influence of deposition periods on the corrosion resistance of multilayer DLC coatings has not been studied so far and there is rarely work on the corrosion behaviors of multilayer DLC coating under various aggressive environments.

In our previous work, Si doped multilayer DLC coatings have been successfully prepared by the plane hollow cathode plasma enhanced chemical vapor deposition (PHC-PECVD) method, exhibiting excellent tribological performance and corrosion resistance.[12,17] Thus, the present work is undertaken in order to studying the effect of deposition periods and corrosive medium (3.5 wt% NaCl, 1 M H_2SO_4, 1 M HCl, 1 M NaOH) on the corrosion resistance of multilayer DLC coatings.

2. Experimental details

The multilayer DLC coatings with different deposition periods were deposited by a PHC-PECVD method (one deposition period consists of one Si_x-DLC layer and one Si_y-DLC layer; Si_x-DLC: low-Si-doped DLC layer, Si_y-DLC: high-Si-doped DLC layer). The substrates used for each deposition were 304 stainless steels (30 mm × 30 mm × 1 mm) and (1 0 0) Si wafers (30 mm × 20 mm × 0.625 mm). The major chemical compositions of 304 stainless steel are 0.06 wt% C, 19.02 wt% Cr, 10.12 wt% Ni and balance Fe. More details about this deposition process had been discussed in our previous work.[12]

[a]State Key Laboratory of Solid Lubrication, Lanzhou Institute of Chemical Physics, Chinese Academy of Sciences, Lanzhou 730000, China. E-mail: lpwang@licp.cas.cn; qjxue@lzb.ac.cn; Fax: +86 931 4968163; Tel: +86 931 4968080

[b]Key Laboratory of Marine Materials and Related Technologies, Ningbo Institute of Materials Technology and Engineering, Chinese Academy of Sciences, Ningbo 315201, China

[c]University of Chinese Academy of Sciences, Beijing 100039, China

† Electronic supplementary information (ESI) available. See DOI: 10.1039/c6ra05527c

Substrates were cleaned ultrasonically in acetone and ethanol for 20 min, respectively. Then they were placed under vacuum chamber. Before the coating deposition, the vacuum chamber was evacuated to a base pressure (1.5×10^{-3} Pa), and high pure argon (Ar) gas (150 sccm, 1.5 Pa) was introduced to sputter the substrates (−5 kV, 30 min) to remove the surface contaminants. The Si transition layer was fabricated to obtain better adhesion at −15 kV (frequency 1.5 kHz, duty cycle 30% and deposition time 15 min) and the pressure was 15 Pa, with high pure argon and silane (SiH_4) gas flow of 100 and 50 sccm, respectively. The multilayer DLC coatings (alternate Si_x-DLC and Si_y-DLC layers) with different deposition periods were grown on the substrates at a bias voltage of −0.8 kV with a mixture of acetylene (C_2H_2) and silane (SiH_4) as precursor gases. The Si_x-DLC layer and Si_y-DLC layer could be deposited periodically on the substrate by adjusting the flow of acetylene (C_2H_2). Four multilayer DLC coatings with different deposition periods are considered in this study. Table S1 in ESI† lists the detailed deposition parameters.

Field scanning electron microscope (FESEM, S-4800, HITACHI) was employed to investigate the surface and cross-section morphology of the multilayer DLC coatings. The chemical depth profile of the coatings was analyzed by the time-of-flight secondary-ion mass spectrometry (ToF-SIMS) measurement with a ToF-SIMS IV instruments using 30 keV Bi^+ primary ions. Atomic force microscopy (AFM, CSPM4000, Benyuan, China) was used to obtain the surface roughness of the coatings. The electrochemical measurements were performed to evaluate the corrosion behaviors of the multilayer DLC coatings in corrosive solution. The conventional three electrode cell was used to carry out the electrochemical study, consisting of a saturated calomel electrode (SCE, 0.241 V *versus* standard hydrogen electrode) as reference electrode, a Pt sheet as counter electrode and the sample with 0.5 cm^2 exposed area as working electrode. Prior to electrochemical measurements, multilayer DLC coating was first immersed in corrosive solution for 30 min to achieve a steady open circuit potential. Potentiodynamic polarization tests were conducted at a scan rate of 10 mV s^{-1}. Electrochemical impedance spectroscopy (EIS) tests were measured at the open circuit potential with an AC amplitude of 10 mV over the frequency range from 100 kHz to 10 mHz. Salt spray test was carried out to evaluate the long-term corrosion resistance using machine (KW-ST-60), according to KS D 8334 standard.[18] In the whole process, chamber temperature was set to 35 °C and air saturator temperature was set to 47 °C. Immersion test was performed under various corrosive solutions for 168 h at room temperature. The exposed area of the coating was 2.54 cm^2. The chemical compositions and X-ray photoelectron spectroscopy of the coatings as deposited and after 168 h immersion were examined using a Thermo Scientific ESCALAB 250Xi instrument equipped with a monochromatic Al Kα (1486.8 eV) X-ray source. Binding energies were calibrated using the C 1s peak (284.8 eV). Among them, samples using 304 stainless steel as substrate were used for electrochemical characterization, salt spray test and immersion test. The samples using (1 0 0) Si wafers as substrate were used for microscopic observations of coating microstructures.

3. Results and discussion

3.1. Microstructure and composition of the multilayer DLC coatings

Fig. 1 shows the cross-section images of Si-doped multilayer DLC coatings. The coating consists of a cyclical layer composed of Si_x-DLC and Si_y-DLC. The total thickness of the multilayer DLC coatings is approximately 15.3, 10.7, 9.7 and 10.0 μm, respectively, and the corresponding deposition periods for four multilayer DLC coatings are 5, 12, 15, and 20, respectively.

Fig. 2 presents the depth profiles of elements in multilayer DLC coatings (taking the coating with 5 and 20 periods as examples) by the ToF-SIMS measurement. This method is based on sputtering the atomic layers from the coating surface by the bombardment of primary ion.[19,20] The coating is mainly composed of the elements of C, Si, O and H. In this paper, we focused on the depth analysis of several "secondary ions" (C_2H^-, CH^-, CH_2^-, Si^-, SiC^-, SiH^-, H^- and O^-) belonging to the coating. The production of the negative "secondary ions" are mainly attributed to the ionization of the atoms and molecules by the interaction of the primary beam composed of positively charged ions and the coating surface.[19,20] In contrast with Si_y-DLC layer, it can be seen that Si_x-DLC layer is characteristic with higher intensity of carbon and hydrogen "secondary ions" (C_2H^-, CH^-, CH_2^- and H^-) and lower intensity of silicon and oxygen "secondary ions" (Si^-, SiC^-, SiH^-, H^- and O^-). This demonstrates that Si_x-DLC layer has lower Si content than Si_y-DLC layer. In addition, depth distribution for these negatively "secondary ions" also give a clear elemental demarcation between the Si_x-DLC and Si_y-DLC layers, verifying the periodic multilayer structure and distinct interface of DLC coatings observed by FESEM.

It was reported that the addition of Si could contribute to the formation of insulating Si oxides in the coating surface, increasing the coating's impedance.[21] Therefore, it is clear from Fig. 2 that oxygen exists throughout the whole coating and the intensity of O^- in Si_y-DLC layer is higher than that in Si_x-DLC layer. And this phenomenon is consistent with our previous XPS

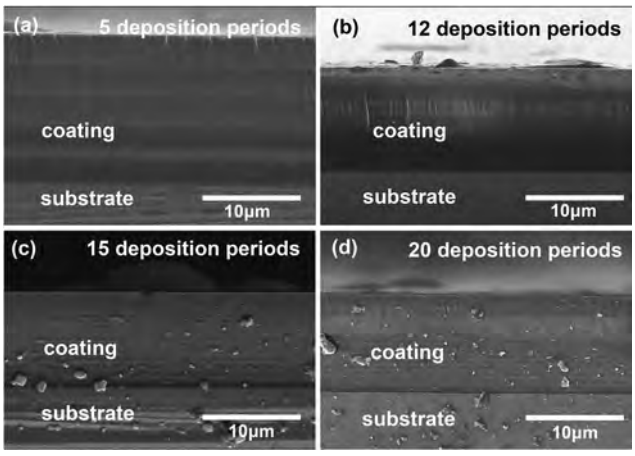

Fig. 1 The SEM images of the cross-section of multilayer DLC coatings with different deposition periods.

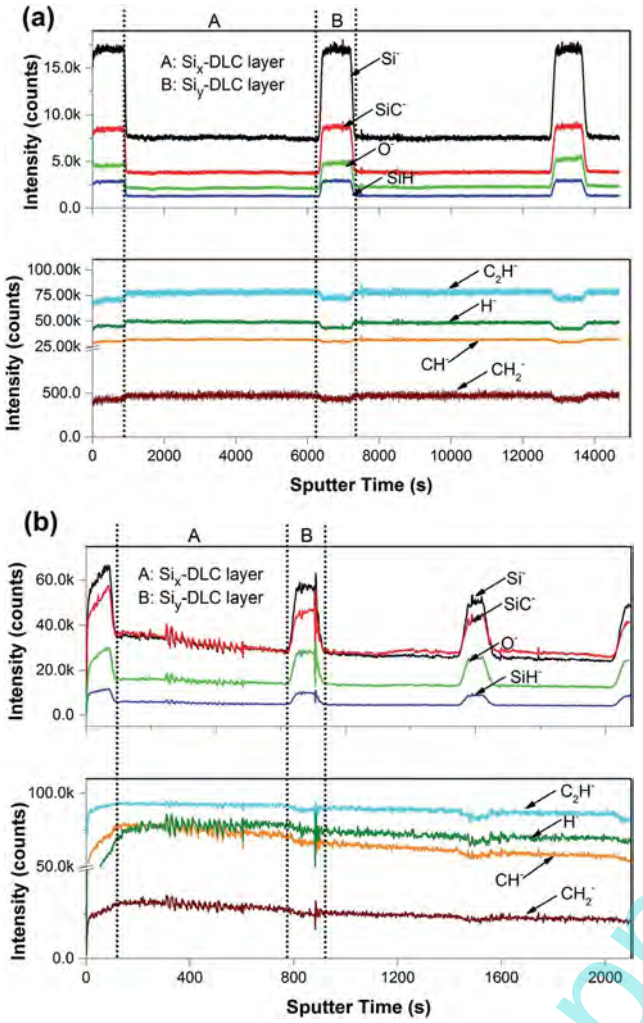

Fig. 2 Depth profile analysis of the multilayer DLC coatings. (a) 5 deposition periods, (b) 20 deposition periods.

analysis (: 82.3 atom% C, 7.1 atom% Si, and 7.1 atom% O for Si$_x$-DLC layer; 71.4 atom% C, 10.7 atom% Si, and 14.8 atom% O for Si$_y$-DLC layer).[12] In addition, the incorporation of Si can cause an opening up of the sp^2 rings and the decrease of the sp^2 cluster size, and increase the content of sp^3 bonds, thus improving the coatings' corrosion resistance.[22] The presence of SiC$^-$ indicates the bonding of C and Si. The formation of Si–C bond in the coating can dramatically relieve stress in a longer-range order and improve the adhesion strength between the coating and substrate due to the difference in the bond lengths between Si–C (1.89 Å) and C–C (1.54 Å).[12,23]

Fig. 3 presents the SEM surface morphologies of the multilayer DLC coatings with different deposition periods. The surface morphologies are very smooth and dense. All coatings have droplets on the surfaces that are typical for the plasma enhanced CVD process. Fig. S1 in ESI† shows the surface roughness of multilayer DLC coatings. It can be seen from Fig. 3 and S1† that the surface morphology has hardly difference among the multilayer coatings with different deposition periods. In general, the surface smoothness and roughness are closely related with the bias voltage, gas pressure, Si concentration and duty cycle during the deposition process. However, in this experiment, all the deposition conditions mentioned above are same for the multilayer DLC coating and the top layer is Si$_y$-DLC for all coatings. Consequently, we can conclude that deposition periods have little effect on the surface morphology and roughness.

3.2. Corrosion behaviors of the multilayer DLC coating with different deposition periods

The potentiodynamic polarization plots of the multilayer DLC coatings in 3.5 wt% NaCl solution are shown in Fig. 4. The corrosion potential (E_{corr}) and corrosion current density (i_{corr}) calculated from the Tafel extrapolation are summarized in Table 1. It can be observed from Fig. 4 and Table 1 that all multilayer DLC coatings are almost equal in the corrosion current density. However, it can be found that the anodic corrosion current density decreases with the increase of deposition periods, and the coating with higher deposition periods has lower anodic polarization curve throughout the whole potential range. This indicates that the coating with higher periods provides better anodic corrosion protection. In addition, the corrosion potentials E_{corr} of the coatings with 5, 12, 15 and 20 deposition periods are about −0.19 V, −0.16 V, −0.11 V and −0.038 V, respectively. A shift in the E_{corr} towards more noble value for the coating with 20 deposition periods (−38 mV) is apparent, compared to those of the coating with 5, 12 and 15 deposition periods. It is reported that the higher the corrosion potential is, the more difficult the corrosion process occurs.[2] This also suggests that the highest deposition periods results in the better corrosion resistance. The superior corrosion resistance of multilayer DLC coating results from the interface effect which can inhibit the growth of defects and retard the penetration of corrosive medium into the substrate.[13]

Owing to the slight variation in the corrosion current density for the different coatings, the EIS measurements were conducted to further investigate the corrosion behaviors of multilayer DLC coatings. The EIS results of the multilayer DLC coatings after an initial time of 30 min exposure in 3.5 wt% NaCl solution are presented in Fig. 5 in the form of Nyquist and Bode plots. It can be clearly seen from Fig. 5a that the Nyquist plots of multilayer DLC coatings with different deposition periods are characterized by a capacitive loop at the high and intermediate frequencies, and a linear component at the low frequencies region. The capacitive loop is associated with the corrosion resistance of the coatings. In general, the larger the capacitive loop is, the better the corrosion resistance of the coating is.[13] It can be observed that the diameter of semicircle of the coating progressively increases with the increase of deposition periods and the multilayer DLC coating with 20 deposition periods has the largest diameter of semicircle. The linear component at the low frequencies corresponds to the Warburg impedance, indicating that the diffusion process occurs in the multilayer DLC coatings.[24–26] This diffusion process can be attributed to the transport of electrolyte through the defects and cracks within multilayer interface. It is evident from Fig. 5b that

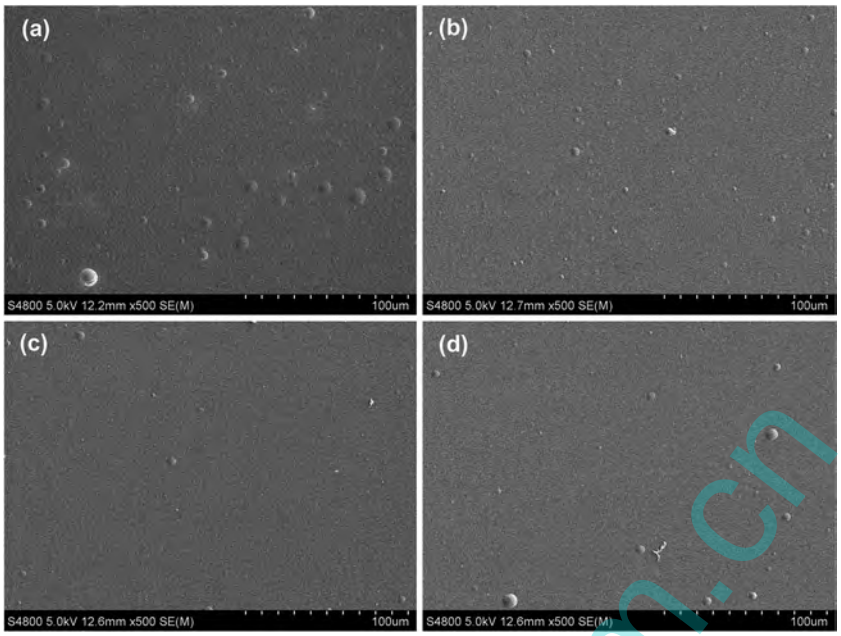

Fig. 3 SEM images of surface morphology of multilayer DLC coatings. (a) 5 deposition periods, (b) 12 deposition periods, (c) 15 deposition periods, (d) 20 deposition periods.

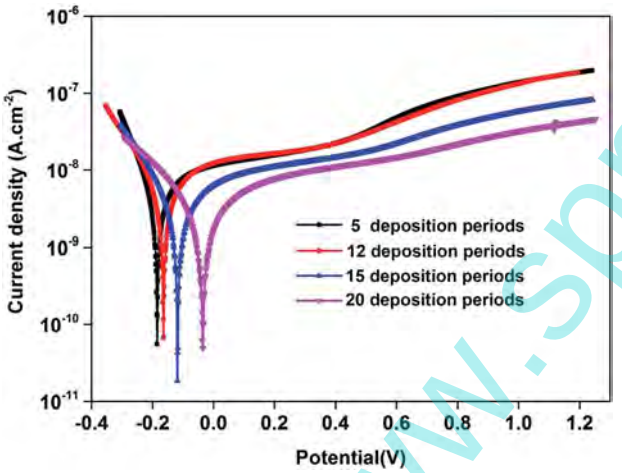

Fig. 4 Potentiodynamic polarization plots of the multilayer DLC coatings with different deposition periods in 3.5 wt% NaCl solution.

Table 1 Electrochemical parameters for the potentiodynamic polarization plots of the multilayer DLC coatings with different deposition periods

Deposition periods	E_{corr} (V)	i_{corr} (10^{-9}A cm^{-2})
5	−0.19	6.6
12	−0.16	9.2
15	−0.11	6.0
20	−0.038	7.4

most of the phase angles exceed 45°. Nishikata *et al.*[27] have reported that the model of the current distribution can be estimated from EIS. When the frequency is scanned from high to low, the current distribution is considered homogeneous if the phase angle is higher than 45° at least in the lower frequency region.[28] Thus, the current distribution in the coating in these EIS tests can be considered uniform.

In addition, Bode plots (frequency *versus* phase angle, Fig. 5b) for all samples were characterized with two time constants: one time constant at the high frequencies referring to the capacitive response of multilayer DLC coatings, and the second at low frequencies corresponding to the diffusion process of electrolyte in the multilayer DLC coating. To analyze the impedance data of the multilayer DLC coating, an equivalent electrical circuit depicted in Fig. 5c was employed. In the equivalent circuit, R_s is the solution resistance, R_c and CPE_c represent the resistance and capacitance of the multilayer DLC coating. The presence of the CPE is due to distributed surface reactivity, surface heterogeneity, roughness or fractal geometry, electrode porosity and to current and potential distributions related with electrode geometry.[29] It is defined by admittance Y and power index number n, given by $Y = Y_0(j\omega)^n$.[30] The CPE has been considered to represent a circuit parameter with limiting behavior as a capacitor for $n = 1$, a resistor for $n = 0$, and an inductor for $n = -1$.[31] In all cases of this investigation, n is close to 1, represents capacitive characteristic of the interfaces. W_1 is the Warburg impedance which indicates partial control of corrosion by the diffusion of electrolyte within the multilayer DLC coating.[32] The general formula is $Y(W) = Y_0(j\omega)^{1/2}$ and $n = 1/2$.[30] Corresponding fitting results of the circuit elements are summarized in Table 2. It can be seen from the fitting data that the values of R_c and W_1 increase evidently with the increasing deposition periods of multilayer DLC coatings. This behavior implies that the coating with more interfaces (higher deposition periods) exhibits higher corrosion resistance, which

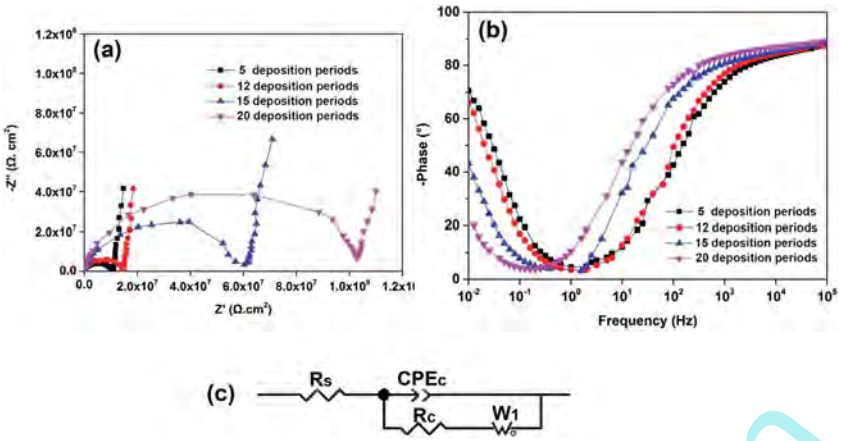

Fig. 5 EIS results of multilayer DLC coatings with different deposition periods in 3.5 wt% NaCl solution. (a) Nyquist plots, (b) Bode plots (frequency *versus* phase angle), (c) the equivalent circuit of R(Q(RW)) model.

is attributed to the reduced quantity of pinholes and the prolonged diffused path of corrosive medium by increasing the number of interfaces.[13] Therefore, the coating with 20 deposition periods presents the best corrosion resistance, which is in agreement with the potentiodynamic polarization results shown in Fig. 4.

However, the EIS results obtained in the short exposure time (30 min) is not sufficient to reveal the protective performance of the multilayer DLC coating. Thus, to investigate whether the coatings can also serve as an anticorrosion coating in 3.5 wt% NaCl solution over a much longer time scale, the coatings with different deposition periods were placed inside the salt spray chamber for 720 h. Fig. S2 in ESI† presents the macroscopic photographs of the samples after the 720 h salt spray test. However, there is not very different in the corroded appearance between four samples. Therefore, EIS test was carried out to obtain the variation in impedance values of four coatings after 720 h salt spray test. The impedance value at low frequencies ($|Z|_{f=0.01\ \mathrm{Hz}}$) in the Bode plot is always used to evaluate the corrosion resistance of the coatings.[25,33] The higher the value of $|Z|_{f=0.01}$ is, the higher the corrosion resistance is.[25] Fig. 6 presents the Bode plots of four coatings before and after 720 h salt spray test. It can be found that there seems to be a downward trend for the impedance values of all coatings after 720 h salt spray test while only the impedance value for the coating with 20 deposition periods shows a slight decrease. This trend is consistent with the above investigation and demonstrates that the multilayer DLC coating with 20 deposition periods holds the best long-term corrosion resistance in 3.5 wt% NaCl solution.

Table 2 Parameter analysis of EIS results for the multilayer DLC coatings with different deposition periods

Deposition periods	R_c (Ω cm^2)	CPE$_c$ (Ω^{-1} cm^{-2})	n	W_1 (Ω cm^2)
5	9.4×10^6	3.3×10^{-10}	0.91	5.5×10^6
12	1.3×10^7	2.8×10^{-10}	0.92	4.4×10^6
15	5.5×10^7	2.1×10^{-10}	0.92	2.4×10^7
20	9.4×10^7	2.2×10^{-10}	0.93	4.1×10^7

In general, DLC coatings may always contain some open pores or closed pores that allow the corrosive medium to diffuse in the coating. For the coating with less interfaces (*e.g.* single layer DLC coating), the vertical propagation was usually preferred for the defects till penetrating to the substrate due to

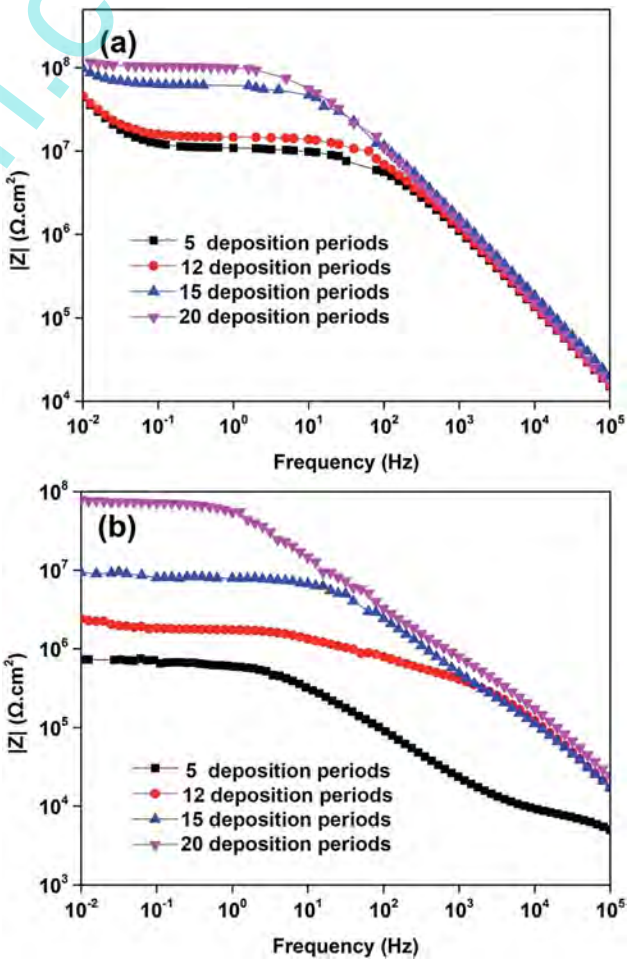

Fig. 6 Bode plots of the multilayer DLC coating with different deposition periods before (a) and after (b) 720 h salt spray test.

the excellent penetration ability of Cl^-.[34] Once the corrosive medium penetrated into the substrate, the corrosion process happened due to the difference of potential between the coating and substrate, in which the substrate went on to be corroded as anode, while the DLC coatings were not attacked as the cathode. In case of Si doped multilayer DLC coatings, the improvement of corrosion resistance typically results from the multilayer interfaces which possibly locally cover the micro-pores of the layer below and make the electrolyte encounter a more tortuous path in traversing the coatings.[14–16,34] With the increase in interface in coating, the ion transportation path is prolonged or blocked, thus reducing the sensitivity of defects and improving the corrosion resistance of the multilayer DLC coatings.

3.3. Corrosion behaviors of multilayer DLC coating under various corrosive solutions

From the above results we can find that the coating with 20 deposition periods exhibits superior corrosion performance on 304 steel substrate, as determined by electrochemical and salt spray test. Consequently, we take this coating as research object to investigate its corrosion behavior under various corrosive solutions. The potentiodynamic polarization plots of the coating under various corrosive solutions (including 3.5 wt% NaCl, 1 M HCl, 1 M NaOH and 1 M H_2SO_4) are presented in Fig. 7, and the corresponding corrosion potential (E_{corr}) as well as corrosion current density (i_{corr}) are listed in Table 3. It can be observed from Fig. 7 and Table 3 that the corrosion current density of the coating under various corrosive solutions increases in the following order: 3.5 wt% NaCl < 1 M H_2SO_4 < 1 M HCl < 1 M NaOH. Especially, in NaOH solution the corrosion potential of the coating is extremely negative compared to that in neutral and acidic solutions. These observations indicate that the coating has poor corrosion resistance in NaOH solution. In addition, it was reported that SiO_2 and SiC compounds could easily react with hydroxide ion (OH^-) and the possible chemical reaction were listed as follows (1)–(4).[35] The presence of Si–C and Si–O bonds in multilayer DLC coating may cause

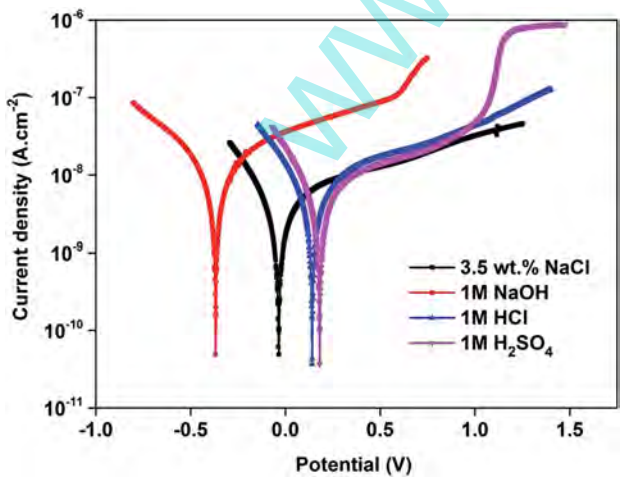

Fig. 7 Potentiodynamic polarization curves of the multilayer DLC coating with 20 deposition periods under various corrosive solutions.

Table 3 Corrosion potential and corrosion current density of the multilayer DLC coatings under various corrosive solutions

Corrosive solutions	E_{corr} (V)	i_{corr} (10^{-9} A cm^{-2})
3.5 wt% NaCl	−0.038	7.4
1 M H_2SO_4	0.19	9.74
1 M HCl	0.14	15.4
1 M NaOH	−0.35	70.8

a series of complex reactions, leading to the poor corrosion resistance in NaOH solution.

$$SiO_2 + 2OH^- \rightarrow SiO_3^{2-} + H_2O \quad (1)$$

$$SiO_3^{2-} + 4H_2O + CO + 6e^- \rightarrow SiC + 8OH^-, \quad E^0 = -1.113\ V \quad (2)$$

$$SiO_3^{2-} + 6H_2O + CO_3^{2-} + 8e^- \rightarrow SiC + 12OH^-, \quad E^0 = -1.141\ V \quad (3)$$

$$SiO_3^{2-} + 3H_2O + C + 4e^- \rightarrow SiC + 6OH^-, \quad E^0 = -1.515\ V \quad (4)$$

EIS results of the coating under various corrosive solutions are presented in Fig. 8 in the form of Nyquist plot. All Nyquist plots exhibit a capacitive loop related to the corrosion resistance of the multilayer DLC coating in high and middle frequencies. Unlike in acidic or neutral solutions, where diffusion process was detected at the low frequencies, in alkaline solution an incomplete arc corresponding to the formation of a double layer of charge at the coating–electrolyte interface was observed.

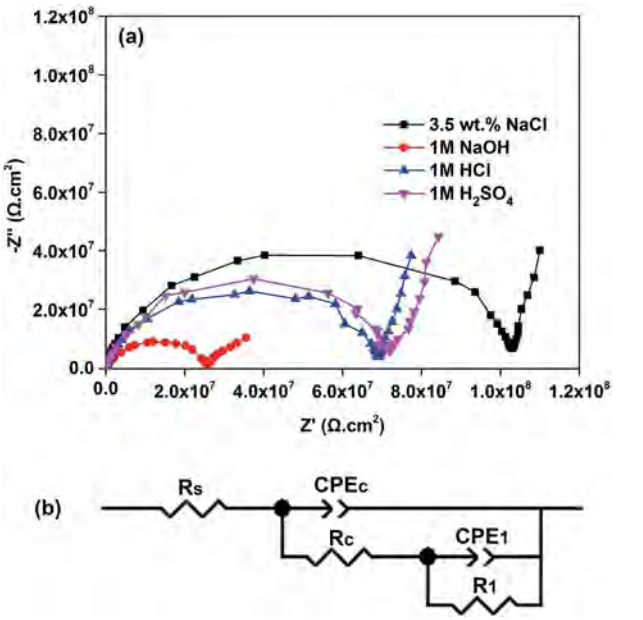

Fig. 8 EIS plots of multilayer DLC coatings with 20 deposition periods under various corrosive solutions. (a) Nyquist plots, (b) equivalent circuit for the multilayer DLC coating in NaOH solution.

To better understand the corrosion behaviors of multilayer DLC coating under various corrosive solutions, two equivalent circuits were employed to fit the EIS results. The first equivalent circuit (Fig. 5c) was used to fit the EIS data displaying a Warburg impedance in acidic and neutral solutions, whereas the second one (Fig. 8b) was used for the EIS data displaying two capacitive loops in alkaline solution. In both equivalent circuits, the meanings of R_s, R_c, CPE_c and W_1 are same with the explanation shown in Fig. 5c. CPE_1–R_1 corresponds to the double layer capacitance and charge transfer resistance. The appearance of double layer capacitance reveals that the corrosion reaction occurs. Table S2 in ESI† summarizes the fitting results obtained from the equivalent circuits. Apparently, the order of the impedance values for the multilayer DLC coating under various corrosive solutions is 3.5 wt% NaCl > 1 M H_2SO_4 > 1 M HCl > 1 M NaOH. This result is in agreement with the polarization results shown in Fig. 7.

Immersion test offers a simple and cheap method to investigate the long-term corrosion resistance of the multilayer DLC coatings immersed in the aggressive environments.[36] In this investigation, immersion test was carried out on the multilayer DLC coatings with 20 deposition periods by immersing them under various corrosive solutions for 168 h at room temperature. After prolonged exposure time, the difference is much more evident. The macroscopic photographs and surface morphologies of samples after the 168 h of immersion are shown in Fig. 9. As can be seen from the images, the coating immersed in 3.5 wt% NaCl and 1 M H_2SO_4 solutions (Fig. 9a and b) has no remarkable changes or less corrosion after 168 h immersion while the entire surface of the coating is severely damaged and detachment is observed for the coating immersed in 1 M HCl solution (Fig. 9c). For the coating immersed in 1 M NaOH solution (Fig. 9d), localized occurrence of the pits probably results from the complex corrosion reactions mentioned above. To further analyze the corrosion causes of the coating under various corrosive solutions, XPS was used to analyze the variation in chemical composition of the surface.

Fig. 10(a)–(e) shows the Si 2p core level spectra from the multilayer DLC coatings as deposited and after 168 h immersion under various corrosive solutions. The spectra are fitted by resolving each into two components with Gaussian line shapes in order to identify the various bonding schemes of silicon. The peaks with bonding energy at 100.5 eV and 102.3 eV correspond to Si–C and Si–O, respectively.[12] As can be seen in Fig. 10(e) and Table 4, the relative intensity of Si–C and Si–O bonds in the coating as deposited isn't much different. However, after 168 h immersion, Si 2p core level spectra in Fig. 10(a)–(d) show that the relative intensity of Si–O is higher than Si–C for all samples. In case of the coating immersed in 3.5 wt% NaCl, 1 M H_2SO_4 and 1 M HCl solutions (Fig. 10a, b and d), the relative intensity

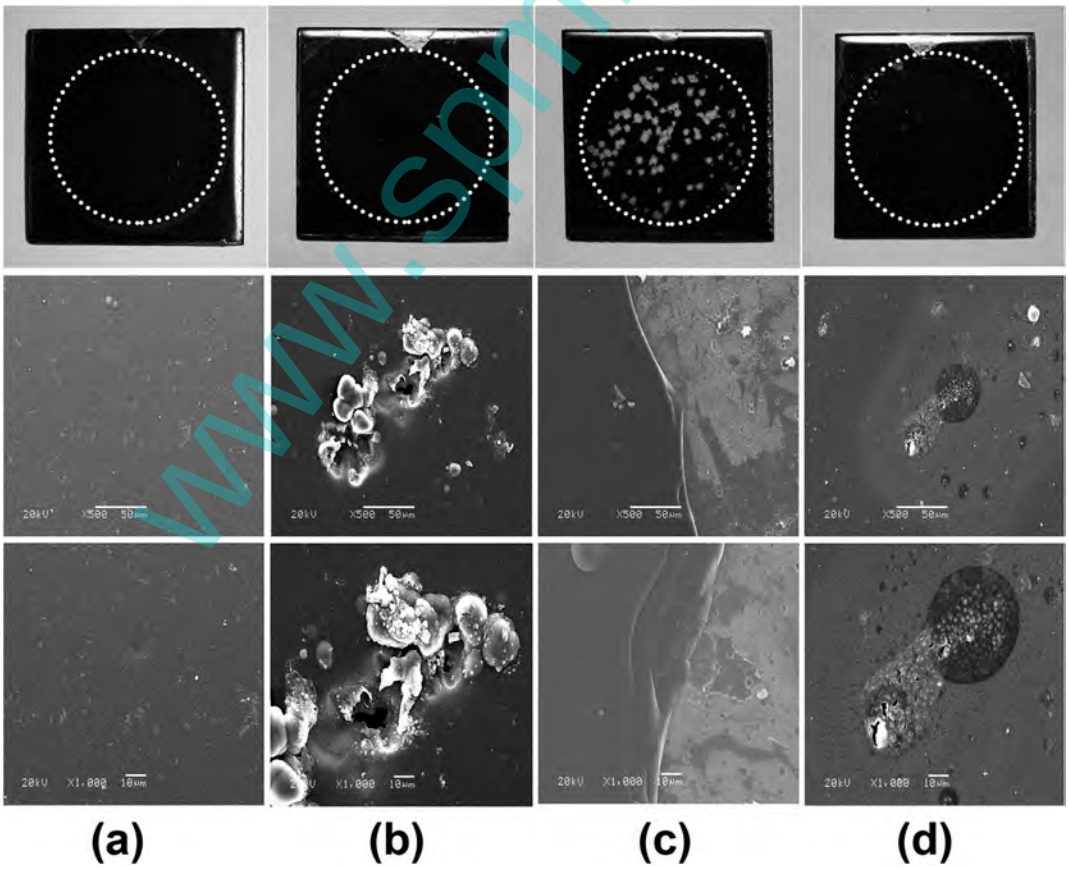

Fig. 9 SEM micrographs of the corroded surface of multilayer DLC coating coated samples after immersion tests under various corrosive solutions. (a) 3.5 wt% NaCl, (b) 1 M H_2SO_4, (c) 1 M HCl, (d) 1 M NaOH. All the tests are conducted for 168 h at room temperature.

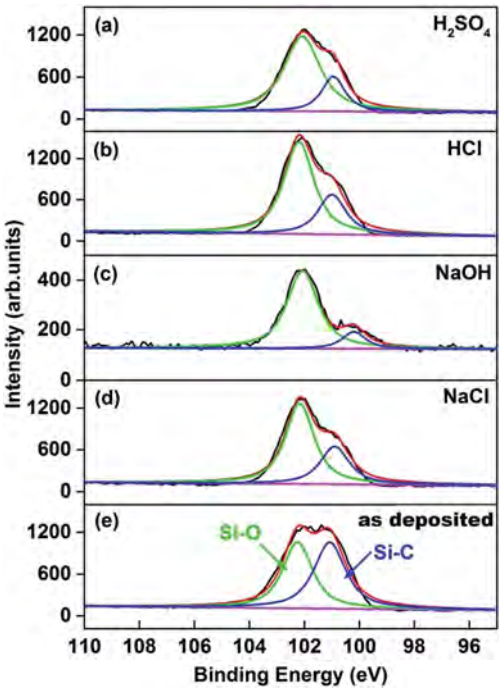

Fig. 10 XPS spectra of Si 2p from multilayer DLC coating as deposited and after 168 h immersion under various corrosive solutions. (a) 1 M H_2SO_4, (b) 1 M HCl, (c) 1 M NaOH, (d) 3.5 wt% NaCl, (e) as deposited.

Table 4 The surface chemical composition of multilayer DLC coating as deposited and after 168 h immersion under various corrosive solutions

Corrosive solutions	C (at%)	Si (at%)	O (at%)
As deposited	68.6	13.5	17.9
3.5 wt% NaCl	69.6	12.2	18.2
1 M HCl	68.0	13.4	18.6
1 M H_2SO_4	69.3	11.4	19.3
1 M NaOH	80.0	3.3	16.7

of Si–O bond increases while the relative intensity of Si–C bond decreases, with the coating as deposited as a comparison. This may be attributed to the surface oxidation and etching of multilayer DLC coating. In addition, it can be observed from Table 4 that the contents of Si, C and O after immersion test have small changes. However, the detachment has occurred for the coating immersed in 1 M HCl solution. Consequently, we can conclude that the multilayer DLC coating is relatively stable in 3.5 wt% NaCl and 1 M H_2SO_4 solutions and sensitive to HCl solution. This reveals that reaction activity of the Cl^- is possibly enhanced in acidic environments, thus accelerating the corrosion process and leading to the delamination of multilayer DLC coatings. The multilayer DLC coatings may always contain some pores or cracks which allow some specific ions or molecules in the electrolyte to gradually migrate to the substrate surface.[37] When the electrolyte accesses the coating surface, the pores or cracks in the coating become the initiation sites of the corrosion and continue to expand. Generally, multilayer DLC coating is electrochemically noble when compared to steel substrate. With the increase in immersion time, electrolyte gradually permeated into the substrate through the pores or defects within the coating and a galvanically induced corrosion can occur between the coating and the substrate, thus resulting in the detachment of coating from substrate.[32,36] For the coating immersed in alkaline solution, the relative intensity of Si–O and Si–C bonds decrease dramatically compared to the coating as deposited, and the content of Si shown in Table 4 also show a significant decrease. This indicates that corrosion may come from the complex reactions of the Si element with the OH^- ions in the electrolyte.

4. Conclusions

The multilayer DLC coating with different deposition periods was fabricated using PHC-PECVD method. The effects of deposition periods and corrosive medium on the corrosion behaviors of the multilayer DLC coating were systematically investigated using potentiodynamic polarization, EIS, salt spray test and immersion test. The results show that the corrosion resistance of multilayer DLC coatings improves with the increasing deposition periods and the multilayer DLC coating with 20 deposition periods exhibits the better corrosion resistance in 3.5 wt% NaCl solution. In addition, variable corrosion behaviors were found for multilayer DLC coating under various corrosive solutions, in which the coating exhibits stable corrosion resistance in 3.5 wt% NaCl and 1 M H_2SO_4 solutions while poor resistance in the 1 M HCl and 1 M NaOH solutions. This is possibly attributed to the enhanced reaction activity of the Cl^- in acidic environments and the complex chemical reaction between the coating and active species.

Acknowledgements

The authors gratefully acknowledged financial support provided by the National Key Basic Research Program (No. 2014CB643302) and National Natural Science Foundation of China (Grant No. 51322508). The authors also gratefully acknowledged Prof. Jun Wang for performing electrochemical measurements.

References

1 F. Li, S. Zhang, J. Kong, Y. Zhang and W. Zhang, *Thin Solid Films*, 2011, **519**, 4910–4916.
2 A. S. Hamdy, *Electrochim. Acta*, 2011, **56**, 1554–1562.
3 Z. Xu, Y. J. Zheng, F. Jiang, Y. X. Leng, H. Sun and N. Huang, *Appl. Surf. Sci.*, 2013, **264**, 207–212.
4 Z. Xu, H. Sun, Y. X. Leng, X. Li, W. Yang and N. Huang, *Appl. Surf. Sci.*, 2015, **328**, 319–324.
5 Z. M. Wang, J. Zhang, X. Han, Q. F. Li, Z. L. Wang and R. Wei, *Corros. Sci.*, 2014, **86**, 261–267.
6 R. Sharma, P. K. Barhai and N. Kumari, *Thin Solid Films*, 2008, **516**, 5397–5403.
7 Y. Uematsu, T. Kakiuchi, T. Teratani, Y. Harada and K. Tokaji, *Surf. Coat. Technol.*, 2011, **205**, 2778–2784.

8 L. Joska and J. Fojt, *Appl. Surf. Sci.*, 2012, **262**, 234–239.
9 D. Bootkul, B. Supsermpol, N. Saenphinit, C. Aramwit and S. Intarasiri, *Appl. Surf. Sci.*, 2014, **310**, 284–292.
10 L. A. Dobrzanski, K. Lukaszkowicz, D. Pakula and J. Mikula, *Arch. Comput. Mater. Sci. Surf. Eng.*, 2007, **28**, 12–18.
11 J. Choi, M. Kawaguchi, T. Kato and M. Ikeyama, *Microsyst. Technol.*, 2007, **13**, 1353–1358.
12 J. Wang, J. Pu, G. Zhang and L. Wang, *ACS Appl. Mater. Interfaces*, 2013, **5**, 5015–5024.
13 G. H. Song, X. P. Yang, G. L. Xiong, Z. Louand and L. J. Chen, *Vacuum*, 2013, **89**, 136–141.
14 C. Liu, A. Leyland, Q. Bi and A. Matthews, *Surf. Coat. Technol.*, 2001, **141**, 164–173.
15 L. A. Dobrzański, K. Lukaszkowicz, A. Zarychta and L. Cunha, *J. Mater. Process. Technol.*, 2005, **164**, 816–821.
16 C. Liu, P. K. Chu, G. Lin and D. Yang, *Corros. Sci.*, 2007, **49**, 3783–3796.
17 M. Cui, J. Pu, J. Liang, L. Wang, G. Zhang and Q. Xue, *RSC Adv.*, 2015, **5**, 104829–104840.
18 C. Lee, A. Kim and J. Kim, *Surf. Coat. Technol.*, 2015, **264**, 127–131.
19 A. Benninghoven, *Surf. Sci.*, 1994, **299**, 246–260.
20 A. M. Belu, D. J. Graham and D. G. Castner, *Biomaterials*, 2003, **24**, 3635–3653.
21 P. Papakonstantinou, J. F. Zhao, A. Richardot, E. T. McAdams and J. A. McLaughlin, *Diamond Relat. Mater.*, 2002, **11**, 1124–1129.
22 J. Choi, M. Kawaguchi, T. Kato and M. Ikeyam, *Microsyst. Technol.*, 2007, **13**, 1353–1358.
23 T. Takeshita, Y. Kurata and S. J. Hasegawa, *Appl. Phys.*, 1992, **71**, 5395.
24 S. Chen, P. Wang and D. Zhang, *Corros. Sci.*, 2014, **87**, 407–415.
25 R. Li, J. Liang, Y. Hou and Q. Chu, *RSC Adv.*, 2015, **5**, 60698–60707.
26 G. Yılmaz, G. Hapçı and G. Orhan, *J. Mater. Eng. Perform.*, 2015, **24**, 709–720.
27 R. V. Cruz, A. Nishikata and T. Tsuru, *Corros. Sci.*, 1996, **38**, 1397–1406.
28 X. Liao, F. Cao, L. Zheng, W. Liu, A. Chen, J. Zhang and C. Cao, *Corros. Sci.*, 2011, **53**, 3289–3298.
29 F. Rosalbino, E. Angelini, D. Macciò, A. Saccone and S. Delfino, *Electrochim. Acta*, 2009, **54**, 1204–1209.
30 C. Liu, Q. Bi and A. Matthews, *Corros. Sci.*, 2001, **43**, 1953–1961.
31 J. B. Jorcin, M. E. Orazem, N. Pébère and B. Tribollet, *Electrochim. Acta*, 2006, **51**, 1473–1479.
32 J. Liang, P. B. Srinivasan, C. Blawert and W. Dietzel, *Corros. Sci.*, 2009, **51**, 2483–2492.
33 J. Liang, P. B. Srinivasan, C. Blawert and W. Dietzel, *Corros. Sci.*, 2010, **52**, 540–547.
34 D. Chen, N. Jin, W. Chen, L. Wang, S. Zhao and D. Luo, *Surf. Coat. Technol.*, 2014, **254**, 440–446.
35 M. Herrmann, K. Sempf, H. Wendrock, M. Schneider, K. Kremmer and A. Michaelis, *J. Eur. Ceram. Soc.*, 2014, **34**, 1687–1693.
36 N. W. Khun, E. Liu and X. T. Zeng, *Corros. Sci.*, 2009, **51**, 2158–2164.
37 A. Zeng, E. Liu, I. F. Annergren, S. N. Tan, S. Zhang, P. Hing and J. Gao, *Diamond Relat. Mater.*, 2002, **11**, 160–168.